

Unsteady Flow in Cavitating Turbopumps

J. H. KIM

Research Associate,
Applied Research Laboratory,
The Pennsylvania State University,
State College, Pa.

A. J. ACOSTA

Professor,
Dept. of Mechanical Engineering,
California Institute of Technology,
Pasadena, Calif.

Unsteady flow in a cavitating axial inducer pump is analyzed with the help of a simple two-dimensional cascade model. This problem was motivated by a desire to study the effect of unsteady cavitation on the so-called POGO instability in the operation of liquid rocket engines. Here, an important feature is a closed loop coupling between several different modes of oscillation, one of which is due to the basic unsteady characteristics of the cavitation itself. The approaching and leaving flow velocities up- and downstream of the inducer oscillate, and the cavity-blade system participates dynamically with the basic pulsating flow. In the present work, attention is focused on finding a transfer matrix that relates the set of upstream variables to those downstream. This quantity, which is essentially equivalent to cavitation compliance in the quasi-static analyses, is found to be complex and frequency dependent. It represents the primary effect of the fluctuating cavity in the system. The analysis is based on a linearized free streamline theory.

Introduction

The problem of unsteady internal cavitating flows such as frequently observed in a pump or a turbine has drawn renewed attention recently in connection with its role played in the so-called POGO instability during the operation of liquid propellant rockets. This kind of system instability typically arises during the booster stage of flight, and is attributed to a feedback coupling between the cavitating feed pump, the supporting structure, and the motion of the propellant in the feed lines to the pump. Naturally, because of this rather complicated situation due to the coupling effect, the problem has remained somewhat unexplored in its full essence. For instance, although it is generally believed that the unsteady behavior of the cavitation itself is of essential importance to the problem, it is only very recently that an attempt was made to incorporate this into the problem [1, 2].¹

Some of the earlier pioneering works on this subject by Rubin [3, 4], Fashbaugh and Streeter [5], and Ghahremani [6] adopted the following typical assumptions in order to make the problem more treatable:

First, a passive "compliance" is attributed to the presence of cavitation in the pump, that is, the presence of cavitation is visualized as acting like a pressurized reservoir, and numerical values for the pump cavitation compliance are determined from dynamic experiments, or test stand firings, to make the observed frequencies match the theoretical ones;

Secondly, the behavior of the pump during the unsteady mo-

tions of the transient flow is assumed to be quasisteady, namely, the change in pump performance parameters with flow rate and inlet pressure is assumed to be the same as that corresponding to steady state operation.

Brennen and Acosta [7] used this quasisteady line of approach in analyzing cavitating cascade. This type of analysis may be a correct one for a first step, and if the frequencies of oscillation were sufficiently low, the quasisteady representation of the pump performance might prove to be satisfactory. On the other hand, it should be pointed out that the inherent unsteadiness of the cavitation is not taken into account in these works, in spite of the fact that this fluctuating behavior of the cavity is an important source of system instability.

The unsteady characteristics of a cavity flow have been considered in a recent study by Kim and Acosta [1] using a simple dynamic model of a base-cavitating wedge in a tunnel, and it was concluded that the quasisteady analysis was not adequate for a wide range of frequencies of oscillation. In the present work, we will treat an unsteady flow through a cavitating axial inducer pump using the linearized free streamline theory. The inducer can be represented by a two-dimensional cascade model.

Formulation of the Problem

Consider a two-dimensional unsteady flow past a cavitating inducer cascade as sketched in Fig. 1. Let us assume the cascade blades to be flat plates, semi-infinite in length, with a stagger angle of γ . The steady angle of incidence α will be supposed to be small; the cavity is assumed to be slender so that it may be represented as a slit along the vane. The flow is approximated to be incompressible, inviscid, and irrotational. Far upstream, there exists only an axial velocity fluctuation approaching the inducer denoted by \tilde{V}_{1e}^{in} and no tangential velocity fluctuation. Far downstream, the flow must be parallel to the vanes, and for

¹Numbers in brackets designate References at end of paper.

Contributed by the Fluids Engineering Division and presented at the Cavity Flow Symposium, Minneapolis, Minn., May 5-7, 1975, of THE AMERICAN SOCIETY OF MECHANICAL ENGINEERS. Manuscript received at ASME Headquarters, February 5, 1975.

this reason both the normal or axial ($\tilde{N}_2 e^{j\omega t}$) and the tangential ($\tilde{T}_2 e^{j\omega t}$) fluctuations will prevail. It is also assumed that the whole flow system oscillates at a single frequency ω .

Now, in the absence of the body-cavity system, elementary dynamic principles may be applied to calculate the difference in fluctuating pressures between any two remote points in the flow in terms of the pulsating velocity components. The primary effect of inserting the unsteady cavity-blade system (which interferes dynamically with the flow) is then to alter the pressure at these remote points by additional amounts $\tilde{P}_1 e^{j\omega t}$ and $\tilde{P}_2 e^{j\omega t}$ respectively for the given velocity disturbances.

Our objective here is to determine these residuary pressures \tilde{P}_1 and \tilde{P}_2 in terms of the fluctuating velocity components for given flow geometry and frequency so that ultimately we may be able to relate the four quantities (\tilde{P}_1 , \tilde{P}_2) and (\tilde{N}_1 , \tilde{N}_2) by

$$\begin{pmatrix} \tilde{P}_1 \\ \tilde{P}_2 \end{pmatrix} = cM \begin{pmatrix} \tilde{N}_1 \\ \tilde{N}_2 \end{pmatrix} \quad (1)$$

where M is a 2×2 matrix and c is a factor that nondimensionalizes M . M is equivalent to a transfer matrix that relates the upstream conditions to the downstream ones.

The cavity terminus will be assumed fixed. This artificial assumption will make the unsteady and the steady flow problems separable, and is justifiable only because we are interested in the overall volume fluctuation due to the cavity and not in the local behavior of the cavity length variation.

Solution of the Problem

Let us denote the velocity components in the x - and the y -directions by $U + u$ and v , respectively, where $|u|/U$, $|v|/U \ll 1$.

On the cavity, the linearized Euler's equation in the x -direction gives

$$\frac{\partial u}{\partial t} + U \frac{\partial u}{\partial x} = 0.$$

Writing the perturbation velocity $u = u_c + u_c(x)e^{j\omega t}$ on the cavity, one finds $u_c(x) = ge^{-jkx/d}$. Here, $k \equiv \omega d/U$ is reduced frequency and g is a constant to be determined from the solution. Along the vanes outside the cavity, $v = 0$. The linearized z -plane is shown in Fig. 2 with appropriate boundary conditions.

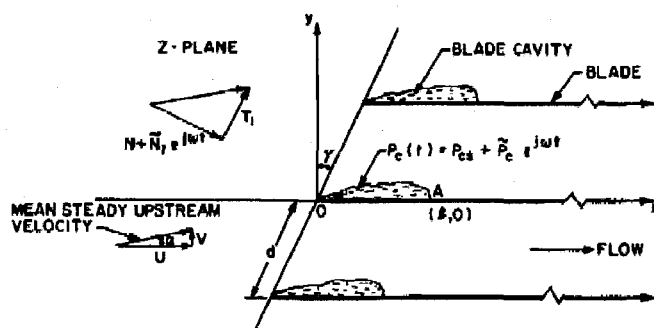


Fig. 1 Sketch of unsteady flow through cavitating cascade

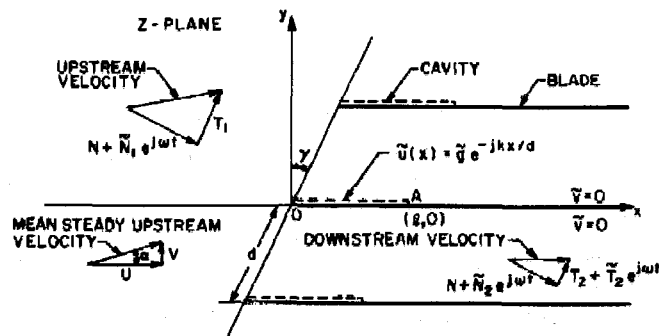


Fig. 2 Linearized z -plane with boundary conditions

The complex perturbation velocity $w = u - iv$ is an analytic function of $z = x + iy$ at each instant by incompressibility and irrotationality.

To find the solution for w , it is convenient to map the linearized z -plane into the upper half of an auxiliary plane by the following transformation [8, 9]:

$$z = \frac{d}{2\pi} \left[e^{-i\gamma} \ln(1 - \zeta/\zeta_1) + e^{i\gamma} \ln(1 - \bar{\zeta}/\bar{\zeta}_1) \right] \quad (2)$$

in which the branch point $\zeta_1 = \sqrt{d} e^{i(x/2 - \gamma)}$ corresponds to upstream infinity in the z -plane. Writing $w = w_s(\zeta) + w(\zeta)e^{j\omega t}$

Nomenclature

d = blade spacing along cascade axis
 i = unit imaginary number with regard to space
 j = unit imaginary number with respect to time, $ij \equiv -1$
 k = reduced frequency, $\omega d/U$
 l = cavity length
 M = transfer matrix
 N = steady velocity normal to cascade axis
 N_1 = unsteady upstream perturbation velocity normal to cascade
 N_2 = unsteady downstream perturbation velocity normal to cascade
 P_1 = residuary pressure at far upstream
 P_2 = residuary pressure at far downstream
 S = abscissa of cavity terminus in the ζ -plane
 T_1 = steady upstream velocity tan-

gential to cascade axis
 T_2 = steady downstream velocity tangential to cascade axis
 \tilde{T}_2 = unsteady downstream perturbation velocity tangential to cascade axis
 u = perturbation velocity in the x -direction
 U = steady upstream velocity in the x -direction
 \tilde{u} = unsteady part of perturbation velocity in the x -direction
 v = perturbation velocity in the y -direction
 \tilde{v} = unsteady part of perturbation velocity in the y -direction
 w = complex perturbation velocity ($w = u - iv$)
 \tilde{w} = unsteady part of complex perturbation velocity ($\tilde{w} = \tilde{u}$

$- iv$)
 z = complex variable in the physical plane, $z = x + iy$
 α = steady angle of attack at upstream infinity
 γ = stagger angle of cascade axis
 ρ = fluid density
 σ = cavitation number
 ω = angular velocity of oscillation
 ζ = complex variable in the transformed plane, $\zeta = \xi + i\eta$

Subscripts

1, 2 = conditions at upstream and downstream infinity, respectively
 c = conditions on the cavity surface
 s = steady solutions

Superscripts

\sim = unsteady part

where $\tilde{w} = \tilde{u} - i\tilde{v}$, one can establish the boundary conditions for \tilde{u} and \tilde{v} in the ξ -plane as shown in Fig. 3:

$$\begin{aligned} \tilde{v} &= 0, \xi < 0, \eta = 0 \\ \tilde{u} &= \tilde{g}e^{-i\kappa(\xi/d)}, 0 < \xi < s, \eta = 0 \\ \tilde{v} &= 0, \xi > s, \eta = 0 \end{aligned}$$

where

$$\frac{x(\xi)}{d} = \frac{1}{\pi} \left\{ \frac{\cos \gamma}{2} \ln \left(1 - \frac{\xi}{\sqrt{d}} \sin \gamma + \xi^2/d \right) - \sin \gamma \tan^{-1} \frac{-\xi \cos \gamma}{\sqrt{d} - \xi \sin \gamma} \right\}. \quad (3)$$

The solution of this mixed-type Hilbert boundary value problem is readily found to be [10, 11]

$$\tilde{w}(\xi) = \frac{\tilde{g}}{\pi\sqrt{\xi(\xi-S)}} \int_0^s \sqrt{\xi(S-\xi)} e^{-i\kappa(\xi/d)} \frac{d\xi}{\xi-\xi_1} + \frac{A\xi+B}{\sqrt{\xi(\xi-S)}}. \quad (4)$$

Here, \tilde{g} , A , and B are constants (real in space, complex in time) to be determined shortly. S is given from equation (3) by substituting $\xi = S$ and $x(\xi) = l$. The following three conditions are available for the determination of \tilde{g} , A , and B :

(i) At upstream infinity, i.e., as $\xi \rightarrow \xi_1$,

$$\tilde{w} = \tilde{N}_1 \cos \gamma + i\tilde{N}_1 \sin \gamma$$

Equation (4) then gives

$$\frac{\tilde{g}}{\pi\sqrt{\xi_1(\xi_1-S)}} \int_0^s \sqrt{\xi(S-\xi)} e^{-i\kappa(\xi/d)} \frac{d\xi}{\xi-\xi_1} + \frac{A\xi_1+B}{\sqrt{\xi_1(\xi_1-S)}} = \tilde{N}_1 (\cos \gamma + i \sin \gamma). \quad (5)$$

(ii) At downstream infinity, i.e., as $|\xi| \rightarrow \infty$,

$$\tilde{w} = \tilde{N}_2 \cos \gamma + \tilde{T}_2 \sin \gamma + i(\tilde{N}_2 \sin \gamma - \tilde{T}_2 \cos \gamma)$$

Equation (4) thus gives

$$A = \tilde{N}_2 \cos \gamma + \tilde{T}_2 \sin \gamma + i(\tilde{N}_2 \sin \gamma - \tilde{T}_2 \cos \gamma). \quad (6)$$

(iii) Also at far downstream, the flow should be parallel to the vanes. Therefore

$$\tilde{N}_2 \sin \gamma = \tilde{T}_2 \cos \gamma. \quad (7)$$

The foregoing three conditions completely determine \tilde{g} , A , and B , and they can be written

$$\begin{aligned} A &= \tilde{N}_2 / \cos \gamma \\ \tilde{g} &= g_1 \tilde{N}_1 + g_2 \tilde{N}_2 \\ B &= \sqrt{d} (B_1 \tilde{N}_1 + B_2 \tilde{N}_2) \end{aligned} \quad (8)$$

where g_1, g_2, B_1, B_2 are frequency-dependent constants.

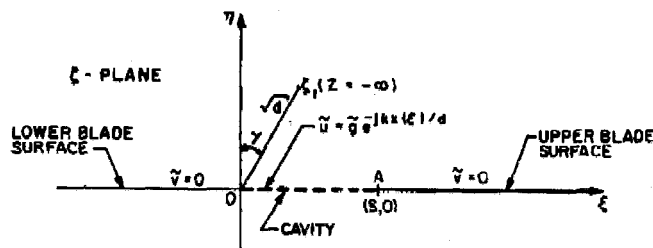


Fig. 3 Transformed plane with linearized boundary conditions

We now proceed to find the relation between (P_1, P_2) and (N_1, N_2) . As $x \rightarrow -\infty$, the Euler's equation of motion gives

$$P \rightarrow -j\omega\rho\tilde{u}_1 x e^{j\omega t} + \tilde{P}_1 e^{j\omega t} + P_{1s} \quad (9)$$

where P_{1s} is the steady mean pressure at upstream infinity, and $\tilde{u}_1 = \tilde{N}_1 \cos \gamma$. Likewise, as $x \rightarrow +\infty$, one may write

$$P \rightarrow -j\omega\rho\tilde{u}_2 x e^{j\omega t} + \tilde{P}_2 e^{j\omega t} + P_{2s} \quad (10)$$

where $\tilde{u}_2 = \tilde{N}_2 \cos \gamma + \tilde{T}_2 \sin \gamma$. Also, writing the x -velocity by $u_s + \tilde{u} e^{j\omega t}$ yields the following linearized equation of motion:

$$\frac{\partial}{\partial t} (u_s + u e^{j\omega t}) + \frac{\partial}{\partial x} \left(\frac{1}{2} u_s^2 + u_s u e^{j\omega t} \right) = -\frac{1}{\rho} \frac{\partial P}{\partial x}.$$

Extracting the unsteady part only, one may write

$$j\omega \tilde{u} + \frac{\partial}{\partial x} (u_s \tilde{u}) = -\frac{1}{\rho} \frac{\partial \tilde{P}}{\partial x}.$$

Integrating this from $(-\infty, 0)$ to $(0^+, 0^+)$, one arrives at

$$U(\sqrt{1+\sigma} \tilde{g} - \tilde{N}_1 \cos \gamma) - j\omega \int_{-\infty}^0 x \frac{d\tilde{u}(x, 0)}{dx} dx = -\frac{1}{\rho} (\tilde{P}_c - \tilde{P}_1). \quad (11)$$

Equation (9) has been applied via the integration by part in the foregoing. Here, \tilde{P}_c is the oscillatory pressure on the cavity and σ is the cavitation number defined by

$$\sigma = \frac{P_{1s} - P_{0s}}{1/2 \rho U^2} \quad (12)$$

where P_{0s} is the steady mean pressure on the cavity.

Similarly, the upstream infinity and the downstream infinity can be related by

$$U[(1 - \tan \alpha \tan \gamma) \tilde{N}_2 / \cos \gamma - \tilde{N}_1 \cos \gamma] - j\omega \int_{-\infty}^0 x \frac{d\tilde{u}(x, 0)}{dx} dx - j\omega \int_0^{\infty} x \frac{d\tilde{u}(x, 0)}{dx} dx = -\frac{1}{\rho} (\tilde{P}_2 - \tilde{P}_1). \quad (13)$$

It can be shown that we may put

$$\int_{-\infty}^0 x \frac{d\tilde{u}(x, 0)}{dx} dx = d(G_1 \tilde{N}_1 + G_2 \tilde{N}_2) \quad (14)$$

$$\int_0^{\infty} x \frac{d\tilde{u}(x, 0)}{dx} dx = d(H_1 \tilde{N}_1 + H_2 \tilde{N}_2) \quad (15)$$

where $G_1, G_2, H_1,$ and H_2 are frequency-dependent constants. Using equations (8), (14), and (15), we can rewrite equations (11) and (13) in the form

$$\vec{P} = M\vec{N} + \vec{P}_c \quad (16)$$

where

$$\vec{P} = \frac{1}{\rho U^2} \begin{pmatrix} \tilde{P}_1 \\ \tilde{P}_2 \end{pmatrix}, \vec{N} = \frac{1}{U} \begin{pmatrix} \tilde{N}_1 \\ \tilde{N}_2 \end{pmatrix}, \vec{P}_c = \frac{\tilde{P}_c}{\rho U^2} \begin{pmatrix} 1 \\ 1 \end{pmatrix}$$

and

$$M = \begin{bmatrix} M_{11} & M_{12} \\ M_{21} & M_{22} \end{bmatrix}$$

$$= \begin{bmatrix} g_1\sqrt{1+\sigma} - \cos\gamma & g_2\sqrt{1+\sigma} - jkG_2 \\ -jkG_1 & \\ g_1\sqrt{1+\sigma} + jkH_1 & g_2\sqrt{1+\sigma} - \frac{1 - \tan\alpha \tan\gamma}{\cos\gamma} \\ & + jkH_2 \end{bmatrix} \quad (17)$$

Thus we have obtained the relation between $(\tilde{P}_1, \tilde{P}_2)$ and $(\tilde{N}_1, \tilde{N}_2)$. The matrix M is a transfer matrix between these two sets of variables. Some numerical values of M are shown in Table 1 for $\alpha = 5$ deg and $\gamma = 75$ deg. The cavitation number σ was obtained from steady-state solution.

Specific Example

As a simple demonstration of how to apply this matrix M to a practical problem, it is interesting to consider an exemplary situation shown in Fig. 4. Here, we have an unsteady cavitating axial inducer pump at the end of a feed pipeline that is connected to a very large reservoir. For simplicity, let us take $P_e = 0$. Assume $L_1/d, L_2/d \gg 1$ where d is the vane spacing of the pump. The pressures on the reservoir surface and the discharge section are given as in the figure. We would like to find the fluctuating

normal velocity components (N_1, N_2) in terms of the given pressures.

The Bernoulli's equation between the reservoir surface and the point A can be written

$$P_{0s} + P_0 e^{j\omega t} + \rho g y_0 = P_{As} + P_A e^{j\omega t} + \frac{\rho}{2} (N + N_1 e^{j\omega t})^2 + \rho \left. \frac{\partial \phi}{\partial t} \right|_A$$

Here, ϕ is the velocity potential. Writing $\phi = \phi_s + \phi e^{j\omega t}$, the unsteady part of the foregoing Bernoulli's equation yields

$$P_0 = P_A + \rho N N_1 + j\omega \rho \phi_A \quad (18)$$

P_A consists of both the residuary part P_1 and the inertial part. To separate them out, let us consider the equivalent cascade problem illustrated in Fig. 5. Here, since L_1 is large, we may approximate by equation (9)

$$P_A(t) \cong j\omega \rho N_1 \cos\gamma (L_1/\cos\gamma) e^{j\omega t} + P_1 e^{j\omega t} + P_{As}$$

so that we may identify

$$P_A = j\omega \rho L_1 N_1 + P_1$$

Substituting this into equation (18) results in

Table 1 Numerical values of M for $\alpha = 5$ deg, $\gamma = 75$ deg

$l/d = 0.01$ ($\sigma = 12.275$)				
h	M_{11}	M_{12}	M_{21}	M_{22}
0	4.308×10^2	-5.365×10^2	4.310×10^2	-5.391×10^2
0.1	4.308×10^2 $+j(1.799 \times 10^{-1})$	-5.365×10^2 $-j(1.788 \times 10^{-1})$	4.310×10^2 $+j(5.629)$	-5.391×10^2 $-j(7.979)$
0.5	4.308×10^2 $+j(8.477 \times 10^{-1})$	-5.363×10^2 $-j(8.940 \times 10^{-1})$	4.310×10^2 $+j(2.814 \times 10)$	-5.390×10^2 $-j(3.989 \times 10)$
0.7	4.308×10^2 $+j(1.260)$	-5.365×10^2 $-j(1.252)$	4.310×10^2 $+j(3.940 \times 10)$	-5.390×10^2 $-j(5.585 \times 10)$
1.0	4.308×10^2 $+j(1.799)$	-5.365×10^2 $-j(1.788)$	4.309×10^2 $+j(5.629 \times 10)$	-5.389×10^2 $-j(7.970 \times 10)$
$l/d = 0.1$ ($\sigma = 2.137$)				
h	M_{11}	M_{12}	M_{21}	M_{22}
0	1.779×10	-3.267×10	1.805×10	-3.528×10
0.1	1.779×10 $+j(6.080 \times 10^{-2})$	-3.267×10 $-j(6.258 \times 10^{-2})$	1.804×10 $+j(3.170)$	-3.526×10 $-j(8.564)$
0.5	1.777×10 $+j(3.039 \times 10^{-1})$	-3.265×10 $-j(3.128 \times 10^{-1})$	1.787×10 $+j(1.585 \times 10)$	-3.496×10 $-j(4.283 \times 10)$
0.7	1.777×10 $+j(4.235 \times 10^{-1})$	-3.265×10 $-j(4.380 \times 10^{-1})$	1.771×10 $+j(2.219 \times 10)$	-3.467×10 $-j(5.996 \times 10)$
1.0	1.777×10 $+j(6.079 \times 10^{-1})$	-3.265×10 $-j(6.258 \times 10^{-1})$	1.737×10 $+j(3.169 \times 10)$	-3.406×10 $-j(8.565 \times 10)$
$l/d = 0.5$ ($\sigma = 0.559$)				
h	M_{11}	M_{12}	M_{21}	M_{22}
0	1.209	-4.575	1.468	-7.177
0.1	1.209 $+j(1.539 \times 10^{-2})$	-4.575 $-j(1.746 \times 10^{-2})$	1.446 $+j(7.381 \times 10^{-1})$	-7.109 $-j(1.138 \times 10)$
0.5	1.207 $+j(7.702 \times 10^{-2})$	-4.567 $-j(8.748 \times 10^{-2})$	9.188×10^{-1} $+j(3.687)$	-5.465 $-j(5.089 \times 10)$
0.7	1.204 $+j(1.079 \times 10^{-1})$	-4.560 $-j(1.227 \times 10^{-1})$	3.906×10^{-1} $+j(5.155)$	-3.819 $-j(7.962 \times 10)$
1.0	1.199 $+j(1.544 \times 10^{-1})$	-4.543 $-j(1.761 \times 10^{-1})$	-7.345×10^{-1} $+j(7.348)$	-3.136×10^{-1} $-j(1.137 \times 10^2)$
$l/d = 1.0$ ($\sigma = 0.111$)				
h	M_{11}	M_{12}	M_{21}	M_{22}
0	7.066×10^{-2}	-5.426×10^{-1}	1.882×10^{-1}	-3.145
0.1	-7.067×10^{-2} $+j(1.041 \times 10^{-2})$	-5.425×10^{-1} $-j(6.660 \times 10^{-3})$	1.660×10^{-1} $-j(2.348)$	-3.081 $-j(4.646)$
0.5	-7.109×10^{-2} $+j(5.209 \times 10^{-2})$	5.414×10^{-1} $-j(3.336 \times 10^{-2})$	3.676×10^{-1} $-j(1.175 \times 10)$	-1.542 $-j(2.321 \times 10)$
0.7	-7.150×10^{-2} $+j(7.295 \times 10^{-2})$	5.402×10^{-1} $-j(4.079 \times 10^{-2})$	-9.038×10^{-1} $-j(1.646 \times 10)$	4.025×10 $-j(3.247 \times 10)$
1.0	-7.239×10^{-2} $+j(1.043 \times 10^{-1})$	-5.376×10^{-1} $-j(6.712 \times 10^{-2})$	-2.052 $-j(2.353 \times 10)$	3.815 $-j(4.631 \times 10)$

